Toxicity and bioaccumulation of sediment-associated silver nanoparticles in the estuarine polychaete, Nereis (Hediste) diversicolor

Cong, Yi; Banta, Gary T.; Selck, Henriette; Berhanu, Deborah; Valsami-jones, Eugenia; Forbes, Valery E.

DOI:
10.1016/j.aquatox.2014.08.001

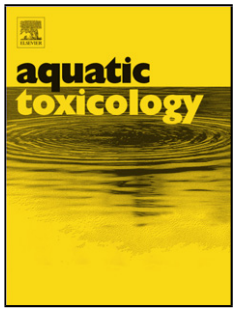

Title: Toxicity and bioaccumulation of sediment-associated silver nanoparticles in the estuarine polychaete, Nereis (Hediste) diversicolor

Author: Yi Cong Gary T. Banta Henriette Selck Deborah Berhanu Eugenia Valsami-Jones Valery E. Forbes

PII: S0166-445X(14)00259-8
DOI: http://dx.doi.org/doi:10.1016/j.aquatox.2014.08.001
Reference: AQTOX 3912

To appear in: *Aquatic Toxicology*

Received date: 4-4-2014
Revised date: 24-7-2014
Accepted date: 3-8-2014

Please cite this article as: Cong, Y., Banta, G.T., Selck, H., Berhanu, D., Valsami-Jones, E., Forbes, V.E.,Toxicity and bioaccumulation of sediment-associated silver nanoparticles in the estuarine polychaete, Nereis (Hediste) diversicolor, *Aquatic Toxicology* (2014), http://dx.doi.org/10.1016/j.aquatox.2014.08.001

Highlights

- Burrowing behavior of *N. diversicolor* was affected after Ag NP exposure.
- Worm size affected Ag bioaccumulation.
- Both Ag forms were cytotoxic and genotoxic to *N. diversicolor* coelomocytes.
- Ag NP treatments were more toxic than aqueous Ag for all toxicity endpoints.
- Enhanced nano-size specific effects warrant further investigation and attention.

Toxicity and bioaccumulation of sediment-associated silver nanoparticles in the estuarine polychaete, *Nereis (Hediste) diversicolor*

Yi Cong [a,b,*], Gary T. Banta [a], Henriette Selck [a], Deborah Berhanu [c], Eugenia Valsami-Jones [c,d], Valery E. Forbes [a,e]

[a] Department of Environmental Social and Spatial Change (ENSPAC), Roskilde University, PO Box 260, 4000 Roskilde, Denmark

[b] National Marine Environmental Monitoring Center, Dalian 116023, China

[c] Department of Mineralogy, Natural History Museum, London SW7 5BD, UK

[d] School of Geography, Earth and Environmental Sciences (GEES), University of Birmingham, Edgbaston, Birmingham, B15 2TT, UK

[e] School of Biological Sciences, University of Nebraska Lincoln, 348 Manter Hall, Lincoln, NE 68588-0118, USA

[*] Corresponding author[1]

Yi Cong

Department of Environmental, Social and Spatial Change (ENSPAC),

Roskilde University,

Universitetsvej 1,

PO Box 260,

4000 Roskilde, DK

Tel: +86 84783171;

Fax: +86 84782586;

E-mail: ycong@nmemc.gov.cn

Email addresses for remaining authors:

Gary T. Banta: banta@ruc.dk ; Henriette Selck: selck@ruc.dk; Deborah Berhanu: d.berhanu@nhm.ac.uk ; Eugenia Valsami-Jones: e.valsami-jones@nhm.ac.uk; Valery E. Forbes: vforbes3@unlnotes.unl.edu

[1] Present address: National Marine Environmental Monitoring Center, Linghe Street 42, Shahekou District, Dalian 116023, Liaoning Province, China

ABSTRACT: In this study, the toxicities of sediment-associated silver added to sediment as commercially available silver nanoparticles (Ag NPs, 20 and 80 nm) and aqueous Ag ($AgNO_3$) to the estuarine polychaete, *Nereis (Hediste) diversicolor*, were investigated for both individual and subcellular endpoints after 10 d of exposure. Both Ag NP types were characterized in parallel to the toxicity studies and found to be polydispersed and overlapping in size. Burrowing activity decreased (marginally) with increasing Ag concentration and depended on the form of Ag added to sediment. All worms accumulated Ag regardless of the form in which it was added to the sediment, and worm size (expressed as dry weight) was found to significantly affect bioaccumulation such that smaller worms accumulated more Ag per body weight than larger worms. Lysosomal membrane permeability (neutral red retention time, NRRT) and DNA damage (comet assay tail moment and tail DNA intensity %) of *Nereis* coelomocytes increased in a concentration-dependent manner in all three Ag treatments. Ag NP treatments were more toxic than aqueous Ag for all toxicity endpoints, even though bioaccumulation did not differ significantly among Ag forms. No significant difference in toxicity was observed between the two Ag NP treatments which was attributed to their overlap in particle size.

KEYWORDS: Silver nanoparticles, sediment exposure, burrowing behavior, Ag body burden, lysosomal membrane stability, DNA damage

1. Introduction

Rapidly expanding growth in nanotechnology has led to the development of numerous applications of nanomaterials in industrial and consumer products. Silver nanoparticles (Ag NPs) are one of the most commonly used nanomaterials, largely due to their enhanced antibacterial properties (Klaine et al., 2008; Luoma, 2008). Engineered Ag NP-containing products, such as odor resistant textiles, household appliances and medical devices are likely to release Ag NPs or ions, via wastewater discharge, into the aquatic environment. The subaquatic environment, sediment, is potential one of the biggest pools of NPs after their agglomeration and sedimentation. Although we know little about realistic concentrations of NPs in aquatic environments, especially in sediments, some studies have simulated real emission scenarios and predicted NP concentrations in realistic environments. For instance, Hendren et al. (2013) calculated effluent concentrations of Ag NPs in wastewater in Monte Carlo using a model approach, which were below 0.12-0.35 μg/L. The modeled concentrations of Ag NPs in the surface waters of the U.S. are between 0.09 and 0.43 ng/L (Gottschalk et al., 2009).

Although no widely accepted risk assessment strategies for NPs exist (Handy et al., 2008), there are concerns that risk assessments based on particle composition (e.g., ionic Ag) may underestimate risk due to nanoparticle-specific properties, which may increase bioavailability and/or reactivity (Wijnhoven et al., 2009). Ag NPs were shown to be bioavailable for different organisms and were internalized inside cells (Johnston et al., 2010). Ag NPs have been found to cause sublethal phenotypic abnormalities in aquatic vertebrate embryos during development (Asharani et al., 2008; Kim et al., 2013; Laban et al., 2010, Wu and Zhou, 2012) and have been shown to be cytotoxic and genotoxic to different cell types, with effects including membrane damage, oxidative stress, metabolism disruption, DNA damage and apoptosis (Choi et al., 2010; Farkas et al., 2010, 2011; Ringwood et al., 2010; Sr et al., 2010; Baker et al., 2014). Most existing studies of Ag NPs have been conducted on vertebrates (particularly freshwater fish or *in vitro* mammalian cell lines), however, and have primarily focused on water exposure pathways, despite the fact that benthic species may be especially at risk as a result of agglomeration and precipitation of Ag NPs from the water phase into sediment. Based on the few studies conducted on sediment exposure there is indication that non-standard endpoints, such as burrowing behavior, may be particularly important when addressing NP effects (Buffet et al., 2011). In a previous study, we investigated genotoxicity of different Ag forms (i.e., Ag NPs (<100 nm), Ag

microparticles (2-3.5 μm), and aqueous Ag ($AgNO_3$)) added to sediment to the benthic ragworm, *Nereis (Hediste) diversicolor* (Cong et al., 2011). We found that Ag caused DNA damage in *Nereis* coelomocytes, and that this effect was both concentration- and Ag form-dependent. Ag NPs had the greatest genotoxic effect of the three tested Ag forms, and aqueous-Ag was the least genotoxic, indicating that different mechanisms were possibly involved in causing DNA damage by the different Ag forms.

The purpose of the present study was to further investigate the toxic effects of commercially available Ag NPs of smaller nominal sizes added to sediment as 20 (Ag NP_{20}) and 80 nm NPs (Ag NP_{80}), in comparison with aqueous Ag ($AgNO_3$). The estuarine sediment-dwelling ragworm, *N. diversicolor*, was selected as a model organism due to its crucial role for the fate of chemicals in sediments via its particle mixing and irrigation activities (Banta and Andersen, 2003; Mouneyrac et al., 2003). Mortality, burrowing behavior, bioaccumulation, lysosomal membrane stability (neutral red assay) and DNA damage (comet assay) were used as endpoints. Thus this study builds upon our previous work (Cong et al. 2011) by examining two different sizes of commercially available Ag NPs as well as $AgNO_3$, and by including burrowing behavior and lysosomal membrane stability (neutral red assay) as additional endpoints to investigate toxic effects of Ag NPs at both individual and cellular levels. The crystal structure, particle size, shape, hydrodynamic diameter and zeta potential were characterized for both Ag NP types in parallel to toxicity assessment.

2. Materials and methods

2.1. Animal collection and culturing

Adult *N. diversicolor*, with lengths ranging from 5-10 cm (corresponding to 0.02-0.2 g dry weight, dw), were collected in Roskilde Fjord (55°40.710'N, 11°59.120'E) during autumn 2010, and placed in natural sandy sediment (collected from the same site, sieved ≤1 mm) to acclimatize for 2-3 days (15 °C) with aerated natural seawater (from the same site, 15 ‰ salinity) in the laboratory. The water was replaced with filtered natural seawater (<0.2 μm, 15 ‰) while the worms acclimatized for another two weeks. One day before exposure, all worms were carefully picked out of the sediment and placed in clean filtered seawater to empty their guts overnight. During the acclimation and exposure periods, worms were fed natural sieved sediment without additional food supply.

2.2. Characterization of Ag NPs

Ag NP_{20} and Ag NP_{80} (stock # 0478HW and 0476HW, 99.9 %, w/~0.3 % PVP coated) were purchased from NanoAmor (Houston, TX, USA). The identification of crystal structure, particle size, hydrodynamic diameter and zeta potential of both particle types was performed as described in Cong et al. (2011). Briefly, the crystal structure of Ag NP powders was determined using X-ray diffraction (XRD) and data were collected using a Nonius PSD 120 powder diffraction system equipped with a position sensitive detector. The primary particle size was measured using a Hitachi H-7100 transmission electron microscope (TEM, operating at 100 kV). The hydrodynamic diameter (in suspension) and zeta potential (a measure of particle surface charge, which can be used as an indication of suspension stability) were measured using a Zetasizer Nano ZS (Malvern Zetasizer Nano ZS, Malvern, UK), performed on a stock Ag NP suspension that was prepared in deionized water (18.2 Ω, Millipore) by sonication (15 min followed by a 15 min pause, repeated 4 times).

2.3. Sediment preparation

Sandy sediment for all treatments was collected from Roskilde Fjord at the same site as worms. The top few centimeters of the sediment surface were scraped off, sieved to ≤1 mm in the field using natural seawater (15 ‰, pH≈8.0) and frozen at -20 °C until use. Before spiking, the sediment was rinsed with filtered natural seawater, and the background Ag concentration was measured using graphite furnace atomic absorption spectrometry (GFAAS, GTA 120, Varian, Australia) as described in Cong et al. (2011). Briefly, the sediment samples were lyophilized (Christ Alpha 1-2, Osterode, Germany) overnight at -50 °C followed by digestion with 65 % HNO_3, neutralization with 25 % ammonium solution and filtration before GFAAS measurement. Another six aliquots of sediment (around 5 g) were taken for dw/ww ratio and organic matter content measurements.

The Ag stock sediment (nominal concentration: 200 µg Ag/g dw) and exposure sediments (nominal concentrations: 5, 10, 25, 50, 100 µg Ag/g dw sed.) were prepared following Cong et al. (2011). Briefly, the stock sediment was obtained by mixing natural wet sediment with a known amount of the Ag stock suspension/solution. The Ag concentration in the stock sediment was measured before diluting with natural wet sediment to the desired series of exposure concentrations. In addition, PVP-controls (0.3 µg PVP/g dw sed.; corresponding to the highest Ag NP concentration of 100 µg Ag/g dw sed.) were prepared similarly to the Ag sediments by

mixing a known volume of PVP solution into wet sediment to determine effects of the PVP coating alone.

2.4. Experimental setup

All experimental plastic beakers were acid washed (20 % HNO_3) and rinsed once with seawater before use. Natural (control) or Ag-spiked sediment (320 g wet weight, ww) and 600 ml filtered natural seawater were added to each beaker and left for six hours to settle. Following overnight gut emptying in seawater, worms were transferred to beakers (one worm per beaker). Six Ag concentrations were tested for each of the 3 Ag forms (n=5) using a randomized block design. This design allowed sufficient time for the measurements that needed to be conducted on living worms at experimental termination. In detail, a replicate block included 1 replicate from each of the 7 treatments (i.e., 3 Ag forms at 5 concentrations plus 1 control (0 µg Ag/g dw sed.) and 1 PVP control) giving a total of 17 beakers per replicate block. Each block was set up on the same day of the week over the course of one month (n=5 blocks). Experiments were conducted in the dark at 15 ºC, and overlying seawater was renewed with aerated seawater once during the exposure period. Replicate blocks were stopped in the same order that they were set up. Mortality was recorded after exposure, and between 3 to 5 worms for each Ag concentration and form were used for each of the tested endpoints.

2.5. Burrowing test

Burrowing behavior of *N. diversicolor* was investigated following Bonnard et al. (2009), with some modifications. After 10 d of sediment exposure, worms were carefully picked out of their beakers and placed individually in beakers containing 5 cm clean natural wet sediment (≤1 mm) and 100 mL filtered seawater. Worm burrowing positions were recorded every 2 min during 30 min, and the time that it took each worm to become fully buried was recorded.

2.6. Neutral red assay

Lysosomal membrane stability was determined following a modified version of the neutral red assay by Weeks and Svendsen (1996), and the extraction of Nereid coelomocytes was based on the procedure described by De Boeck and Kirsch-Volders (1997) and Lewis and Galloway (2008). After the burrowing test, worms were carefully transferred to clean filtered seawater to empty their guts overnight. A neutral red (toluene red, $C_{15}H_{17}N_4Cl$, cat.# N7005, Sigma-Aldrich, Steinheim, Germany) stock solution (20 mg neutral red powder/1 mL dimethyl sulfoxide; DMSO, Merck, Darmstadt, Germany) was freshly prepared, and a neutral red working solution (10 µL

stock solution/2.5 mL of worm physiological solution; 452.4 mM NaCl, 10.8 mM KCl, 58 mM $MgCl_2 \cdot 6H_2O$, 30.25 mM Na_2SO_4, 11.2 mM $CaCl_2 \cdot 2H_2O$, pH 7.8, adapted for marine annelids) (Wells and Ledingham, 1940), was freshly prepared and changed every hour. Afterwards, 30-50 µL coelomic fluid of *N. diversicolor* was gently extracted into physiological solution for each assay by carefully inserting a 1 ml syringe fitted with a 0.4 mm×20 mm needle (chilled prior to use) into the posterior region of the worm (avoiding the gut). Twenty microlitre of this mixture was placed on a slide where it was mixed with an equal volume of neutral red working solution and covered with a cover slip.

The number of coelomocytes with fully stained cytosol (i.e., exhibiting dye leakage from lysosomes to the cytosol) and unstained cytosol (no leakage) were counted under light microscopy (Laborlux S, Leitz, Portugal, 100× magnification), and the ratio of the two cell types was determined. The ratio was assessed during 2 min of counting every 4-10 min, and observations were stopped when the ratio of cells with fully stained cytosol was greater than 50 % of the total cell number or the observation time exceeded 50 min. This interval was recorded as the neutral red retention time (NRRT).

2.7. Comet assay

The comet assay was performed according to Cong et al. (2011), which was based on the protocol of Singh et al. (1998) and Rank and Jensen (2003). Briefly, coelomic fluid of *N. diversicolor* was gently extracted as described above, mixed with agarose and placed on a fully frosted slide. Slides used as positive controls were exposed to UV light (20 s) from a Ren UV C lamp (253.7 nm, 15 W, Sylvania, Japan). All slides were lysed, electrophoresed and neutralized before staining with ethidium bromide. After staining, the slides were examined under a fluorescence microscope (50×oil immersion objective, Dialux 22EB, Leica, Wetzlar, Germany) with 625× magnification using software from Kinetic Imaging (Comet assay III) and scored blind. The levels of DNA damage were measured as tail moment and tail DNA intensity (%).

2.8. Bioaccumulation

After the coelomic fluid for the above assays was sampled, worms were frozen (-20 ºC) until use. The Ag concentrations in worm tissues were determined using GFAAS. Before digestion of worm tissues, all worms were lyophilized overnight at -50 ºC. Afterwards, each worm was ground into powder, using a mortar and pestle, and the powder was digested and analyzed (GFAAS) as described for sediments. We confirmed the validity of our calibration and analysis

of tissue metal concentration by analyzing a certified biological standard (lobster hepatopancreas, LUTS-1, NRC Canada) with a known Ag concentration. Recovery of the standard reference material averaged 98 ± 0.12 % (mean ± standard deviation, n=15).

2.9. Statistical analyses

Measured Ag sediment concentrations at the start of the experiment were analyzed by one-way analysis of variance (One-way ANOVA) to test for differences among Ag forms. For burrowing time, lysosomal membrane stability and DNA damage, data from exposure treatments (5, 10, 25, 50 and 100 µg Ag/g dw sed.) were analyzed using two-way ANOVA to assess and compare effects of Ag form, concentration and their interaction on tested endpoints. Differences in worm size among treatments were analyzed by two-way ANOVA with Ag form and concentration as factors. For Ag bioaccumulation, data from exposure treatments (5, 10, 25, 50 and 100 µg Ag/g dw sed.) were analyzed using analysis of covariance (ANCOVA) with worm size (dw) as the covariate. Due to the block design (i.e., one replicate per week), replicate was taken into consideration as a blocking factor during ANOVA and ANCOVA analyses to reduce variation in response parameters related to temporal (weekly) variation. One-way ANOVA followed by planned comparisons with a Bonferroni correction was used to assess the effects of exposure concentration, PVP controls and positive controls (one PVP or positive control in each replicate for all three Ag forms) compared to the controls (0 µg Ag/g dw sed., one in each replicate for all three Ag forms) for all experimental endpoints, either with all three Ag treatments considered together or for each Ag treatment separately depending on the results of the test of form effects in the two-way ANOVA above. Differences were considered statistically significant at $p \leq 0.05$ and marginally significant at $0.1 \geq p > 0.05$. All experimental data were tested for homogeneity and normality through examination of residuals. In all cases, data were log-transformed to achieve acceptable homogeneity and normality. All statistical analyses were performed using SYSTAT 13.0 software (Chicago, IL, USA).

3. Results

3.1. Characterization of Ag NPs

Both samples of Ag NPs (as powder) were identified as silver (ICDD 4-783) with very similar crystal structure patterns (Figure S1, supporting information, SI). No other material was detected by XRD. The presence of highly crystalline material was observed (Figure S1, sharp peaks), suggesting the presence of large Ag particles in the primary material. A peak broadening was not

observed between the Ag NP_{20} and Ag NP_{80} suggesting that both samples were well crystallized with a similar degree of crystallinity despite their nominal difference in size. TEM images for Ag NP_{20} and Ag NP_{80} were also similar, with polyhedral-shaped particles (Figure 1C, D) often observed. In addition, complex particles displaying branching structures were commonly found in the Ag NP_{20} sample, which were probably produced from the aggregation of smaller particles by collision upon sonication (such particles were not found when using a shorter sonication time of 5 min). The most common particle size for the Ag NP_{20} sample was approximately 50 nm (Figure 1C), which was different from the size described by the manufacturer (Figure 1A), but these may have been particles that fused during treatment. Smaller sized particles of ~10 nm were also found in the Ag NP_{20} sample, which might represent the primary components of the larger particles; these smaller particles could have formed agglomerates as the suspension droplet was dried on the TEM grid. For the Ag NP_{80} sample, actual particle size ranged from approximately 2-100 nm with most particle sizes also being ~50 nm (Figure 1D) which differed somewhat from the manufacturer's information (Figure 1B). The average hydrodynamic diameters were 187±4 nm and 144±2 nm for Ag NP_{20} and Ag NP_{80} (Figure S2A, SI), respectively. The obtained suspension for both Ag NPs was stable as confirmed by zeta potential values of -39.4±0.5 mV and -42.3±0.3 mV for Ag NP_{20} and Ag NP_{80} (Figure S2B, SI), respectively.

Fig. 1.

3.2. Sediment properties

The dw/ww ratio of natural sandy sediment was 0.77 (n=6), the organic matter content (OMC) was 0.68 % (n=6), and the background Ag concentration was 0.027 µg Ag/g dw sed. (n=3). Measured sediment exposure concentrations of the three Ag forms were close to the nominal concentrations, and did not differ significantly among the three forms (Table 1). The low variability in stock sediment concentrations indicates a homogeneous mixing of Ag in all three treatments. We measured Ag concentration in overlying water in a pilot study and confirmed that less than 0.1 % of Ag in sediment was lost to the water.

Table 1

3.3. Mortality

In all three Ag treatments, six worms (out of a total of 105) in all were found dead after 10 d of sediment exposure, but there was no concentration-dependent mortality.

3.4. Burrowing Behavior

In all three Ag treatments, all but 2 worms (one in each of Ag NP_{80}-10 and aqueous Ag-50) completely burrowed into the clean sediment (category 0) within 30 min upon transfer from the contaminated sediment. The lack of burrowing for these two worms was not related to Ag form or concentration indicating that they were probably in poor condition, and they were therefore removed from further analysis. Burrowing time increased at higher exposure concentrations in the two Ag NP treatments while burrowing in all concentrations of the aqueous Ag treatment was comparable to the control (Figure 2). Both Ag form and replicate significantly affected burrowing time, and concentration had a marginally significant effect. Ag NP_{20}-treated worms were significantly impaired compared to the aqueous Ag treatment. However, there was no interaction between Ag form and concentration on burrowing time (Table 2). PVP did not affect worm burrowing behavior compared to the control (0 µg Ag/g dw sed.).

Fig. 2.

Table 2

3.5. Ag body burden

Silver was bioavailable in all three Ag forms and was accumulated by *N. diversicolor*. Ag body burden increased significantly as a function of exposure concentration but also was affected by worm size (Table 2, Figure 3A and 3B). Worm sizes differed significantly (p<0.001) among exposure concentrations making this bioaccumulation pattern less clear. Notably, worms in 25 and 100 µg Ag/g dw sed. exposures were significantly larger (Figure S3), with concomitant lower bioaccumulation, than those used at the other exposure levels. No significant difference in Ag body burden among the three Ag forms or replicates was observed, nor was there an interaction between Ag form and concentration on bioaccumulation (Table 2). Worms exposed to the PVP control had similar low Ag body burden levels as the control worms (data not shown). The body burden for worms in 100 µg Ag/g dw sed. was significantly higher than the control worms for all three Ag forms (Figure 3A). Figure 3C shows corrected Ag body burdens eliminating the effect of worm size.

Fig. 3.

3.6. Lysosomal membrane stability

The control groups had an average NRRT of around 35 min. The NRRT showed a general decrease with increasing Ag concentration (Figure 4), indicating greater lysosomal membrane

permeability (Figure S4). Form, concentration and replicate significantly affected NRRT with the Ag NP_{20} treated groups having significantly lower (p<0.05) NRRT than the aqueous Ag. The NRRT significantly decreased compared to the control at concentrations of 25, 50 and 100 µg Ag/g dw sed. for Ag NP_{20} and aqueous Ag and at 50 and 100 µg Ag/g dw sed. for Ag NP_{80} (Figure 4). No interaction between Ag form and concentration on NRRT was observed (Table 2). PVP had no significant effect on NRRT compared to the control (Figure 4).

Fig. 4.

3.7. DNA damage

Similar to NRRT, Ag form, concentration and replicate significantly affected tail moment and tail DNA intensity (%). There was no interaction between Ag form and concentration for either tail moment or tail DNA intensity (Table 2). Both parameters increased in a concentration-dependant manner with increasing exposure concentration (Figure 5). The Ag NP_{80} had significantly greater effects and marginally greater effects on tail moment (p<0.05) and tail DNA intensity (%) (p=0.052), respectively, compared to aqueous Ag. In addition, Ag NP_{20} had a marginally greater effect on tail DNA intensity (%) (p=0.097) compared to the aqueous Ag. Tail moment was significantly higher at concentrations of 25, 50 and 100 µg Ag/g dw sed. for Ag NP_{80}, at 50 and 100 µg Ag/g dw sed. for Ag NP_{20} and at 100 µg Ag/g dw sed. for aqueous-Ag compared to the control (Figure 5A). Similarly, tail DNA intensity (%) was significantly higher at concentrations of 50 and 100 µg Ag/g dw sed. for Ag NP_{20} and Ag NP_{80} and at 100 µg Ag/g dw sed. for aqueous Ag compared to the control (Figure 5B). There was no significant effect of PVP on either parameter compared to the control. As expected, the positive controls had significantly higher tail moment and tail DNA intensity compared to the control (Figure 5).

Fig. 5.

4. Discussion

4.1. Ag Characterization

We purchased commercial Ag NPs and prepared stable suspensions in deionized water. The nanoparticles characterized are therefore the particles to which the worms were exposed and not the primary particles as received. We found a clear difference between the manufacturer's product specifications (20 and 80 nm, respectively) and what we measured for the two Ag NP samples. Both samples were polydispersed with wide nano-size ranges, and there was no noticeable difference in the size distribution between the two Ag NP forms. A discrepancy

between measured and manufacturer-reported sizes was also observed by Scown et al. (2010) and by Cong et al. (2011), and we recognize that the sample preparation of the suspensions may have altered the primary particles. Other reasons for the differences may be related to the industrial production process, which often results in polydispersion, or to changes in material properties between synthesis and initial characterization and the particular conditions when utilized (e.g., storage time and conditions, pH, ionic strength, temperature and sonication) (Petersen et al., 2014). For instance, complex particles displaying branching structures were found in the Ag NP_{20} sample, which were probably produced from the aggregation of smaller particles by collision under the external force of sonication in our pretreatment of the stock solutions. This highlights the importance of fully characterizing commercially obtained NPs before using them in experiments.

Ideally, characterization of NPs should be performed under conditions as close as possible to the relevant exposure medium (e.g., sediment in our case). However, due to the lack of available methods for characterizing NPs in such complex media, we only characterized Ag NPs prepared in deionized water, although we recognize that the Ag NPs would have likely undergone additional size or surface chemistry changes, such as oxidation or speciation, when transferred to sediment. Bone et al. (2012) found that speciation patterns of Ag NPs varied significantly as a function of coating types. While GA (gum arabic)-Ag NPs' speciation patterns suggested significantly higher transformation rates, PVP-coated Ag NPs were stable and resisted transformation in sediment (>92.4% Ag (0)) after 24 h, indicating relatively minor effects of oxidation or sulfidation on PVP-coated Ag NPs. Lowery et al. (2012) investigated long-term (18 months) behavior of PVP-coated Ag NPs in freshwater mesocosms simulating an emergent wetland environment. Ag NPs in subaquatic sediment were found present as Ag_2S (55%) and Ag-sulfhydryl compounds (27%), and Ag^+ ions released followed oxidation of Ag NPs could account for only a small part of the total Ag recovered from the sediment. These results indicate that speciation of PVP-coated Ag NPs in sediment can occur, but probably at a relatively slow rate. Also, the speciated forms remained bioavailable (Lowery et al., 2012). Clearly, there is still a pressing need for the improvement of techniques that permit thorough examination of the state and behavior of NPs in complex compartments, such as sediment, so that a better understanding and interpretation of the effects of NPs on organisms can be achieved.

4.2. Difference among replicates

As described above, replicate was treated as a blocking factor in the present study. Replicate was significant for all endpoints tested indicating that there was significant temporal variability in the condition or response of the worms tested during the course of the experiment. Typically one replicate differed significantly from the other replicates, which may be related to the fact that worms were collected on different occasions. Inclusion of the block effect in the study design and analysis separated this source of variability from the treatment comparisons (Ag form, concentration and their interaction) of interest. Ignoring this source of variability would have resulted in much lower sensitivity in the statistical analyses resulting in fewer significant treatment effects.

4.3. Burrowing behavior

Infauna species such as *Nereis diversicolor* are involved in the biogeochemical cycling of nutrients and contaminants through their bioturbation activity. This is strongly linked to their burrowing activity, which is a commonly used indicator of invertebrate behavioral response to sediment toxicity (Boyd et al., 2002). In this study, we use burrowing time instead of 'percent of un-burrowed organisms' (Bonnard et al., 2009) to assess effects of Ag on *Nereis* burrowing. We did observe a tendency of increasing burrowing time with increasing exposure concentration in Ag NP treated worms, especially in the Ag NP_{20} group. In addition, burrowing time was much longer for worms in Ag NP treatments compared to in aqueous Ag treatments (no effect compared to control group), suggesting potentially greater effects of Ag NP than aqueous Ag even after addition to the sediment and that this endpoint is particularly important when considering NP effects. Although $AgNP_{20}$ had a tendency toward greater toxicity with respect to burrowing activity than $AgNP_{80}$, this was not statistically significant, which is consistent with the unexpected overlap in size between the two NP particle types. The trend toward longer burrowing time in the two Ag NP treatments than in the aqueous Ag treatment consistent with the greater effects of Ag NPs than aqueous Ag observed in the neutral red assay and comet assay. Such impairment of burrowing behavior may lead, for example, to ecologically detrimental effects such as increase the susceptibility of sediment-dwelling species to predation.

4.4. Ag bioaccumulation

Although some studies have demonstrated uptake and localization of Ag NPs inside cells (Farkas et al., 2011; Greulich et al., 2011), few of these have quantified the amount of Ag accumulated in whole organisms over time. Our bioaccumulation results demonstrated that Ag was bioavailable

to *N. diversicolor* to the same degree regardless of form added to the sediment. The lack of difference in Ag body burden among Ag treatments, despite differences detected in cellular toxicity indicators, is consistent with our previous study which also showed no difference in bioaccumulation between Ag NPs and aqueous Ag in this species (Cong et al., 2011). These results are also in agreement with García-Alonso et al. (2011), in which the calculated total Ag body burdens of *N. diversicolor* after 10 d of exposure to 250 ng/g dw sediment spiked with Ag NPs (30±5 nm) and aqueous Ag ($AgNO_3$) were similar. As indicated previously (Cong et al, 2011), *N. diversicolor* is tolerant of heavy metal exposure and is able to control its body concentration of certain metals by the induction of physiological detoxification mechanisms, involving the formation of metal-containing extracellular granules, mineralized lysosomes, excretion of metals by exocytosis via coelomocytes, and synthesis and turnover of metal binding proteins, such as metallothioneins (MTs). The low Ag body burden and the lack of difference in Ag body burden among Ag treatments observed in the present study may suggest that detoxification mechanisms are triggered by the presence of Ag in all three treatments in *N. diversicolor* (i.e., regardless of Ag form added) which can have maintained Ag body burdens at similar levels.

We found that worm size significantly influenced Ag body burden in the present study with smaller worms accumulating more Ag per body weight than larger worms (Table 2, Figure 3B, and Figure S3). The highest Ag body burdens were observed at different concentrations for the different Ag forms, but not in a systematic way. The lack of a monotonic bioaccumulation with increasing exposure concentration was surprising given that we observed monotonic relationships in our previous bioaccumulation study (Cong et al., 2011) and with the other endpoints (NRRT and DNA damage) in the present study. This lack of monotonic pattern may in part be due to the wider size range and larger sizes of worms used in this study. In our previous study, all worms had a similar average size of around 0.03 g dw (corresponding to the smallest size we used in the present study) (Cong et al., 2011). In comparison, worms from the two treatments with the largest worm sizes (0.08-0.1 g dw) in the present study (i.e., the 25 and 100 μg Ag/g dw sed.) had markedly lower Ag body burdens (1.3-3.1 and 3.0-6.2 μg/g dw, respectively) compared to the smaller worms used in the previous study (3.6-7.0 and 6.9-9.9 μg/g dw in 25 and 50 μg Ag/g dw sed., respectively) (Cong et al., 2011). Despite efforts to allocate worms of similar sizes to all Ag forms, significant differences in worm size among

concentrations influenced Ag uptake and bioaccumulation. To account for this effect, we corrected for worm size by using size as a covariate (i.e., the regression equation in Figure 3B) to normalize Ag body burden and found that this resulted in a more monotonic relationship (Figure 3C vs. Figure 3A), especially for the aqueous Ag group. Smaller worms have a higher surface area to volume ratio and a higher metabolic rate than larger worms. As demonstrated by Heip and Herman (1979), the weight-specific growth rate of *N. diversicolor* decreased from 0.0415 d^{-1} to 0.0008 d^{-1} when the length of worms increased from 0.25 cm to 7.25 cm (corresponding to ~0.001-0.1 g dw). This could indicate that smaller worms eat more per body weight and as a result, are more susceptible to accumulate sediment-associated Ag than larger worms. These results highlight the importance of correcting for or minimizing body size differences in toxicological studies.

4.5. Cytotoxicity and genotoxicity

Lysosomes have been identified as a particular target site for toxic effects and play an important role in metabolism of various heavy metals (Moore, 1990). Decreased lysosomal membrane stability (or increased permeability) is thought to be a general measure of stress. The mechanism causing this alteration in membrane stability may involve direct effects of chemicals on the membrane or an increased frequency of secondary lysosome formation in toxicant-stressed cells (Huggett et al., 1992, Weeks and Svendsen, 1996).

The concentration-dependent reduction in NRRTs observed in the coelomocytes of *N. diversicolor* in our study indicated stress resulting from exposure to Ag in sediment. Dose-dependent lysosomal destabilization was also observed in adult oysters (*Crassostrea virginica*) when they were exposed to Ag NP (15±6 nm) concentrations of 0.016 to 16 µg/L for 48 h (Ringwood et al., 2010). Our study confirms that lysosomes of worm coelomocytes are a subcellular target for the action of both particulate and aqueous Ag. Furthermore, Ag NPs tended to have greater lysosomal toxicity than aqueous Ag. Aqueous Ag is known to be accumulated as non-toxic deposits of silver-sulphur granules in lysosomes (Kristiansen et al., 2008; Lansdown, 2007). The specific transport system has been characterized by Havelaar et al. (1998) and involves a heavy metal ion transport protein in the lysosomal membrane which facilitates the uptake of silver through a typical carrier-mediated process. For Ag NPs, García-Alonso et al. (2011) have characterized cellular internalization of Ag NPs (30±5 nm) in gut epithelia of *N. diversicolor*, and found that clusters of electron dense particles resembling Ag nanoparticles

deposited in the lysosomes. In addition, TEM images in their study showed that the lysosomal membrane seemed to break down after 10 d of sediment exposure to 250 ng Ag/g dw sed. in *N. diversicolor*. The uptake of Ag NPs into lysosomes has also been observed in human cell lines (Asharani et al., 2009; Greulich et al., 2011), where uptake was suggested to be through clathrin-dependent endocytosis and macropinocytosis (Greulich et al., 2011). The different transport pathways into lysosome suggests potentially different toxic modes involved in lysosomal toxicity between Ag NPs and aqueous Ag.

Comet assay results demonstrated that Ag caused DNA damage in *N. diversicolor* coelomocytes regardless of the Ag form added to the sediment, which is consistent with existing studies of the genotoxicity of Ag particles/ions in different cell systems (Ahamed et al., 2008; Asharani et al., 2009; Choi et al., 2010; Hidalgo and Dominguez, 1998). Similar to our previous DNA damage data (Cong et al., 2011), both tail moment (2.8) and tail DNA intensity (17.3 %) in controls (0 μg/g dw) demonstrated similar values as those reported by Asharani et al. (2009) (tail moment of ~0.5 to 2.5 in human lung fibroblast cells and glioblastoma cells) and Lewis and Galloway (2008) (% DNA in the tail of ~13 % in *N. diversicolor* coelomocytes), respectively. Worms in this study exposed to 5, 10, 25 and 50 μg Ag/g dw sed. had comparable results with our previous DNA study for both parameters (Cong et al., 2011). In addition, tail moments in 25, 50 and 100 μg Ag/g dw sed. Ag NP exposure groups after 10 d of sediment exposure were also comparable to those of human glioblastoma cells after 48 h exposure to 25, 50 and 100 μg/mL Ag NPs (6-20 nm in size) (Asharani et al., 2009).

The potential mechanisms leading to genotoxicity of Ag NPs likely include binding with DNA strands directly, or ROS-induced damage and Ag^+ ion release (Cong et al., 2011). Aqueous Ag (as Ag^+ ions) has been shown to cause DNA damage by covalently binding with DNA (Hossain and Huq, 2002) and inhibiting DNA synthesis directly (Hidalgo and Dominguez, 1998). In reality, most of the aqueous Ag is not present as free Ag^+ ions after addition into marine sediment, due to speciation and complexation with ligands, e.g., chloride and sulfide. However, despite silver speciation or complexation in marine environments, silver still maintains substantial bioavailability and toxicity (Luoma et al., 1995). Ho et al. (2010) demonstrated that the oxidative dissolution of Ag NPs in the presence of PVP can occur (the Ag NPs used in our study had a w/~0.3 % PVP coating). Although we did not measure Ag^+ ions released from Ag NPs during sediment exposure in our study, our results suggest that the cytotoxicity and

genotoxicity of Ag NPs could not be solely attributed to Ag^+ ion release, as we observed a trend of greater effect in Ag NP treatments compared to the aqueous Ag treatment. Similarly, our previous study also found a significantly greater genotoxicity of Ag NPs (<100 nm) compared to aqueous Ag ($AgNO_3$) (Cong et al., 2011), which suggests that either different mechanisms may be involved in Ag NP and aqueous Ag toxicity or that there are different degrees of reactivity of the different Ag forms in causing DNA damage. Furthermore, García-Alonso et al. (2011) demonstrated separate routes of cellular internalization and differing *in vivo* fates of Ag delivered in NP and dissolved forms, and found significantly larger fractions of Ag NPs than aqueous Ag in the organelles of *N. diversicolor*, suggesting potentially higher cellular toxicities of Ag NPs than aqueous Ag. In addition to the above-mentioned possible mechanisms, Ag NPs may also destroy the membrane integrity of cellular organelles, such as lysosomes (which are involved in metal detoxification) and then indirectly cause genotoxicity. Also, Ag NPs may provide an internal source of Ag^+ ions in a Trojan-horse mechanism (Luoma, 2008) that differs in bioavailability to externally available ionic or soluble Ag. However, García-Alonso et al. (2011) suggested that dissolution of the Ag NPs, either externally or internally, was not important over a time scale of 10 d of sediment exposure in *N. diversicolor,* as metallothionein-like proteins (MTLPs) were found associated with aqueous Ag but were absent in worms after Ag NP treatment. Clearly, further investigations are needed to determine the behavior and long-term transformation of Ag NPs under sediment exposure (either externally or internally) and their mechanisms to cause toxicity in sediment.

In summary, burrowing behavior of *N. diversicolor* tended to be affected after Ag NP exposure, especially in the Ag NP_{20} treatment. Ag was bioavailable and accumulated in worms regardless of form added to sediment, and worm size affected Ag bioaccumulation such that smaller worms accumulated more Ag per body weight than larger worms. We also confirmed that lysosomes of *N. diversicolor* coelomocytes were potential targets for Ag. Both lysosomal membrane permeability and DNA damage of *Nereis* coelomocytes increased in a concentration-dependent manner in all three Ag treatments. We concluded that Ag NP treatments were more toxic than the aqueous Ag for all tested endpoints even though bioaccumulation was similar among forms, indicating that toxicity cannot be estimated based on worm body burden alone. Such enhanced nano-size specific effects in sediment environment warrant further investigation and attention.

Acknowledgements

This work was funded by Roskilde University (RUC), Denmark and the China Scholarship Council (CSC). The research leading to these results has also received funding from the European Union Seventh Framework Programme (FP7/2007-2013) under grant agreement n° 214478 (NanoReTox). The authors gratefully acknowledge Janeck Scott-Fordsmand, Anne-Grete Winding, Klara Jensen, Anja Holden Damsholt, Anne Busk Faarborg and Rikke Guttesen for their technical guidance and assistance during experiments, and Stephen Klaine and Poul Bjerregaard for their comments on an earlier draft of the manuscript.

Conflict of interest

None.

Appendix A. Supplementary data

Additional information about X-ray diffraction pattern, hydrodynamic size distribution and zeta potential of Ag NP_{20} and Ag NP_{80}, average sizes of *N. diversicolor* in the three Ag treatments, and pictures of lysosomes with varying degrees of permeability is available free of charge via the Internet.

References

Ahamed, M., Karns, M., Goodson, M., Rowe, J., Hussain, S.M., Schlager, J.J., Hong, Y., 2008. DNA damage response to different surface chemistry of silver nanoparticles in mammalian cells. Toxicol. Appl. Pharmacol. 233, 404–410.

Asharani, P.V., Low Kah Mun, G., Hande, M.P., Valiyaveettil, S., 2009. Cytotoxicity and genotoxicity of silver nanoparticles in human cells. ACS Nano 3, 279–290.

Asharani, P.V., Wu, Y.L., Gong, Z.Y., Valiyaveettil, S., 2008. Toxicity of silver nanoparticles in zebrafish models. Nanotechnology 19, 255102–2255107.

Baker, T.J., Tyler C.R., Galloway, T.S. Impacts of metal and metal oxide nanoparticles on marine organisms. Environ. Pollut. 186, 257–271.

Banta, T.G., Andersen, O., 2003. Bioturbation and the fate of sediment pollutants-experimental case studies of selected infauna species. Vie. Milieu. 53, 233–248.

Bone, A., Colman, B., Gondikas, A., Newton, K., Harrold, K., Unrine, J., Klaine, S., Matson, C., DiGiulio, R., 2012. Biotic and abiotic interactions in aquatic microcosoms determine fate and toxicity of Ag nanoparticles: part 2-toxicity and Ag speciation. Environ. Sci. Technol. 46, 6925–6933.

Bonnard, M., Roméo, M., Amiard-Triquet, C., 2009. Effects of copper on the burrowing behavior of estuarine and coastal invertebrates, the polychaete *Nereis diversicolor* and the bivalve *Scrobicularia plana*. Hum. Ecol. Risk. Assess. 15, 11–26.

Boyd, W.A., Brewer, S.K., Williams, P.L. 2002. Altered behaviour of invertebrates living in polluted environments. In: Dell'Omo G (ed), Behavioural Ecotoxicology, pp 293–336. John Wiley and Sons, Chichester, UK.

Buffet P.E., Tankoua O.F., Pan J.F., et al., 2011. Behavioural and biochemical responses of two marine invertebrates *Scrobicularia plana* and *Hediste diversicolor* to copper oxide nanoparticles. Chemosphere 84(1), 166–174.

Choi, J.E., Kim, S., Ahn, J.H., Youn, P., Kang, J.S., Park, K., Yi, J., Ryu, D.Y., 2010. Induction of oxidative stress and apoptosis by silver nanoparticles in the liver of adult zebrafish. Aquat. Toxicol. 100, 151–159.

Cong, Y., Banta, T.G., Selck, H., Berhanu, D., Valsami-Jones, E., Forbes, V.E., 2011. Toxic effects and bioaccumulation of nano-, micron- and ionic-Ag in the polychaete, *Nereis diversicolor*. Aquat. Toxicol. 105, 403–411.

De Boeck, M., Kirsch-Volders, M., 1997. *Nereis virens* (Annelida: Polychaeta) is not an adequate sentinel species to assess the genotoxic risk (comet assay) of PAH exposure to the environment. Environ. Mol. Mutagen. 30, 82–90.

Farkas, J., Christian, P., Gallego-Urrea, J.A., Roos, N., Hassellöv, M., Tollefsen, K.E., Thomas, K.V., 2011. Uptake and effects of manufactured silver nanoparticles in rainbow trout (*Oncorhynchus mykiss*) gill cells. Aquat. Toxicol. 101(1), 117–125.

Farkas, J., Christian, P., Urrea, J.A., Roos, N., Hassellöv, M., Tollefsen, K.E., Thomas, K.V., 2010. Effects of silver and gold nanoparticles on rainbow trout (*Oncorhynchus mykiss*) hepatocytes. Aquat. Toxicol. 96(1), 44–52.

García-Alonso, J., Khan, F.R., Misra, S.K., Turmaine, M., Smith, B.D., Rainbow, P.S., Luoma, S.N., Valsami-Jones, E., 2011. Cellular internalization of silver nanoparticles in gut epithelia of the estuarine polychaete *Nereis diversicolor*. Environ. Sci. Technol. 45, 4630–4636.

Gottschalk, F., Sonderer, T., Scholz, R.W., Nowack, B., 2009. Modeled environmental concentrations of engineered nanomaterials (TiO_2, ZnO, Ag, CNT, fullerenes) for different regions. Environ. Sci. Technol. 43, 9216–9222.

Greulich, C., Diendorf, J., Simon, T., Eggeler, G., Epple, M., Köller, M., 2011. Uptake and intracellular distribution of silver nanoparticles in human mesenchymal stem cells. Acta. Biomater. 7, 347–354.

Handy, R.D., Owen, R., Valsami-Jones, E., 2008. The ecotoxicology of nanoparticles and nanomaterials: Current status, knowledge gaps, challenges, and future needs. Ecotoxicology 17, 315–325.

Havelaar, A.C., Gast, I.L., Snijders, S., Beerens, C.E.M.T., Mancini, G.M.S., Verheijen, F.W., 1998. Characterization of a heavy metal ion transporter in the lysosomal membrane. FEBS Lett. 436, 223–227.

Heip, C., Herman, R., 1979. Production of *Nereis diversicolor* O.F. miiller (polychaeta) in a shallow brackish-water pond. Estuar. Coast. Mar. Sci. 8, 297–305.

Hendren, C.O., Badireddy, A.R., Casman, E., Wiesner, M.R., 2013. Modeling nanomaterial fate in wasterwater treatment: Monte Carlo simulation of silver nanopartciles (nano-Ag). Sci. Total Environ. 449, 418–425.

Hidalgo, E., Dominguez, C., 1998. Study of cytotoxicity mechanisms of silver nitrate in human dermal fibroblasts. Toxicol. Lett. 98, 169–179.

Ho, C.M., Yau, S.K., Lok, C.N., So, M.H., Che, C.M., 2010. Oxidative dissolution of silver nanoparticles by biologically relevant oxidants: A kinetic and mechanistic study. Chem. Asian J. 5, 285–293.

Hossain, Z., Huq, F., 2002. Studies on the interaction between Ag^{+} and DNA. J. Inorg. Biochem. 91, 398–404.

Huggett, R.J., Kimerle, R.A., Mehrle, P.M.J., Bergman, H.L., 1992. Biomarkers, biochemical, physiological, and histological markers of anthropogenic stress. Huggett RJ (ed.). Lewis, Boca Raton: FL, U.S.A.

Johnston, H.J., Hutchison, G., Christensen, F.M., Peters, S., Hankin, S., Stone, V., 2010. A review of the in vivo and in vitro toxicity of silver and gold particulates: Particle attributes and biological mechanisms responsible for the observed toxicity. Crit. Rev. Toxicol. 40(4), 328–346.

Kim, K.T., Truong, L., Wehmas, L., Tanguay, R.L., 2013. Silver nanoparticle toxicity in the embryonic zebrafish is governed by particle dispersion and ionic environment. Nanotechnology 24(11), 115101.

Klaine, S.J., Alvarez, P.J.J., Batley, G.E., Fernandes, T.F., Handy, R.D., Lyon, D., Mahendra, S., McLaughlin, M.J., Lead, J.R., 2008. Nanomaterials in the environment: Behavior, fate, bioavailability, and effects. Environ. Toxicol. Chem. 27, 1825–1851.

Kristiansen, S., Ifversen, P., Danscher, G., 2008. Ultrastructural localization and chemical binding of silver ions in human organotypic skin cultures. Histochem. Cell. Biol. 130, 177–184.

Laban, G., Nies, L.F., Turco, R.F,, Bickham, J.W., Sepúlveda, M.S., 2010. The effects of silver nanoparticles on fathead minnow (*Pimephales promelas*) embryos. Ecotoxicology 19, 185–195.

Lansdown, A.B.G., 2007. Critical observations on the neurotoxicity of silver. Crit. Rev. Toxicol. 37, 237–250.

Lewis, C., Galloway, T., 2008. Genotoxic damage in polychaetes: A study of species and cell-type sensitivities. Mutat. Res. 654, 69–75.

Lowry, G.V., Espinasse, B.P., Badireddy, A.R., et al., 2012. Long-term transformation and fate of manufactured Ag nanoparticles in a simulated large scale freshwater emergent wetland. Environ. Sci. Technol. 46: 7027–7036.

Luoma, S.N., 2008. Silver Nanotechnologies and the Environment: Old Problems or New Challenges. Project on Emerging Nanotechnologies. Publication 15. Woodrow Wilson International Center for Scholars and PEW Charitable Trusts, Washington, DC.

Luoma, S.N., Ho, Y.B., Bryan, G.W., 1995. Fate, bioavailability and toxicity of silver in estuarine environments. Mar. Pollut. Bull. 31, 44–54.

Moore, M.N., 1990. Lysosomal cytochemistry in marine environmental monitoring. Histochemistry 22, 187–191.

Mouneyrac, C., Mastain, O., Amiard, J.C., Amiard-Triquet, C., Beaunier, P., Jeantet, A.Y., Simth, B.D., Rainbow, P.S., 2003. Trace-metal detoxification and tolerance of the estuarine worm *Hediste diversicolor* chronically exposed in their environment. Mar. Biol. 143, 731–744.

Petersen, E.J., Henry, T.G., Zhao, J., MacCuspie, R.I., Kirschling, T.L., Dobrovolskaia, M.A., Hackley, C., Xing, B., White, J.C. 2014. Identification and avoidance of potential artifacts and misinterpretations in nanomaterial ecotoxicity measurements. Environ. Sci. Technol. 48: 4226-4246.

Rank, J., Jensen, K., 2003. Comet assay on gill cells and hemocytes from the blue mussel *Mitylus edulis*. Ecotoxicol. Environ. Safe. 54, 323–329.

Ringwood, A.H., McCarthy, M., Bates, T.C., Carroll, D.L., 2010. The effects of silver nanoparticles on oyster embryos. Mar. Environ. Res. 69, S49–51.

Scown, T.M., Santos, E., Johnston, B.D., Gaiser, B., Baalousha, M., Mitov, S., Lead, J.R., Stone, V., Fernandes, T., Jepson, M., Aerle, V.R., Tyler, C.R., 2010. Effects of aqueous exposure to silver nanoparticles of different sizes in rainbow trout. Toxicol. Sci. 115, 521–534.

Singh, N.P., McCoy, M.T., Tice, R.R., Schneider, E.L., 1998. A simple technique for quantitation of low-levels of DNA damage in individual cells. Exp. Cell Res. 175, 184–191.

Sr, J.P.W., Goodale, B.C., Wise, S.S., Craig, G.A., Pongan, A.F., Walter, R.B., Thompson, W.D., Ng, A.K., Aboueissa, A.M., Mitani, H., Spalding, M.J., Mason, M.D., 2010. Silver nanospheres are cytotoxic and genotoxic to fish cells. Aquat. Toxicol. 97, 34–41.

Weeks, J.M., Svendsen, C., 1996. Neutral red retention by lysosomes from earthworm (*Lumbricus rubellus*) coelomocytes: A simple biomarker of exposure to soil copper. Environ. Toxicol. Chem. 15(10), 1801–1805.

Wells, G.P., Ledingham, I.C., 1940. Studies on the physiology of *Arenicola marina* L. II. Accomodations to magnesium concentration in the isolated extrovert. J. Exp. Biol. 17, 353–363.

Wijnhoven S.W., Peijnenburg W.J., Herberts C.A., et al., 2009. Nano-silver – a review of available data and knowledge gaps in human and environmental risk assessment. Nanotoxicology 3(2), 109–138.

Wu, Y., Zhou, Q., 2012. Dose- and time-related changes in aerobic metabolism, chorionic disruption, and oxidative stress in embryonic medaka (*Oryzias latipes*): underlying mechanisms for silver nanoparticle developmental toxicity. Aquat. Toxicol. 124-125, 238–246.

Table 1. Measured (n=3) vs. nominal Ag concentrations in sediment at the start of the experiment.

	Nominal Concentration (µg Ag/g dw sed.)					
	0	5	10	25	50	100
Form	Measured Concentration (µg Ag/g dw sed.) (±SD)					
Ag NP_{20}	0.027 (±0.01)	4.34 (±0.29)	9.57 (±1.88)	27.07 (±2.77)	52.51 (±6.71)	99.83 (±6.16)
Ag NP_{80}		6.27 (±0.28)	11.40 (±0.29)	21.61 (±1.10)	47.57 (±5.84)	95.18 (±3.85)
Aqueous Ag		5.49 (±2.70)	10.98 (±0.69)	23.34 (±1.60)	47.52 (±3.12)	93.18 (±4.03)

Table 2. Statistical comparisons. Effects of Ag form, concentration, Ag form*concentration and replicate (blocking factor) on burrowing time, NRRT and DNA damage were analyzed by two-way ANOVA. Bioaccumulation was analyzed by two-way ANCOVA with replicate as a blocking factor and worm size (dw) as the covariate.

Endpoints	*P*-Value				
	Ag form	Concentration	Ag form*Concentration	Replicate	Worm size
Burrowing time	0.004	0.057	0.650	0.005	-
Bioaccumulation	0.724	0.021	0.939	0.322	<0.001
NRRT	0.017	<0.001	0.127	<0.001	-
Tail moment	0.033	<0.001	0.550	<0.001	-
Tail DNA intensity	0.040	<0.001	0.662	<0.001	-

Figure captions for MS

Fig. 1. TEM images of (A,C) Ag NP_{20} and (B,D) Ag NP_{80}. TEM images of (A) Ag NP_{20} and (B) Ag NP_{80} by NanoAmor. TEM images of (C) Ag NP_{20} and (D) Ag NP_{80} characterized under laboratory condition which demonstrated a polyhedral shape. The major particle size of both Ag NP samples was approximately 50 nm.

Fig. 2. Time for *N. diversicolor* to completely burrow in clean natural sediment after 10 d of exposure to sediment spiked with Ag NP_{20}, Ag NP_{80} or aqueous Ag ($AgNO_3$). The bars represent standard error of the mean (SEM).

Fig. 3. (A) Ag body burden in *N. diversicolor* after 10 d of exposure to sediment spiked with Ag NP_{20}, Ag NP_{80} or aqueous Ag ($AgNO_3$). (B) Linear relationship between worm size and log Ag body burden in *N. diversicolor*. (C) Corrected Ag body burden in *N. diversicolor* according to the regression equation of (B). ** and *** represent significant differences in body burdens of Ag ($p<0.01$ and $p<0.001$, respectively) compared to the control (0 µg Ag/g dw sed.) for all three Ag treatments. Note that there was no significant difference among Ag forms (Table 2); therefore the test of concentration effects versus control was conducted for all three forms together. The bars represent standard error of the mean (SEM).

Fig. 4. Neutral red retention time (NRRT) of *N. diversicolor* coelomocytes after 10 d of exposure to sediment spiked with Ag NP_{20}, Ag NP_{80} or aqueous Ag ($AgNO_3$). ** and *** represent significant differences in NRRT ($p<0.01$ and $p<0.001$, respectively) compared to the control (0 µg Ag/g dw sed.) for each Ag form. The bars represent standard error of the mean (SEM).

Fig. 5. DNA damage of *N. diversicolor* coelomocytes after 10 d of exposure to sediment spiked with Ag NP_{20}, Ag NP_{80} or aqueous Ag ($AgNO_3$). (A) Tail moment. (B) Tail DNA intensity. *, ** and *** represent significant differences ($p<0.05$, $p<0.01$ and $p<0.001$, respectively) compared to the control (0 µg Ag/g dw sed.) for each Ag form. The bars represent standard error of the mean (SEM).

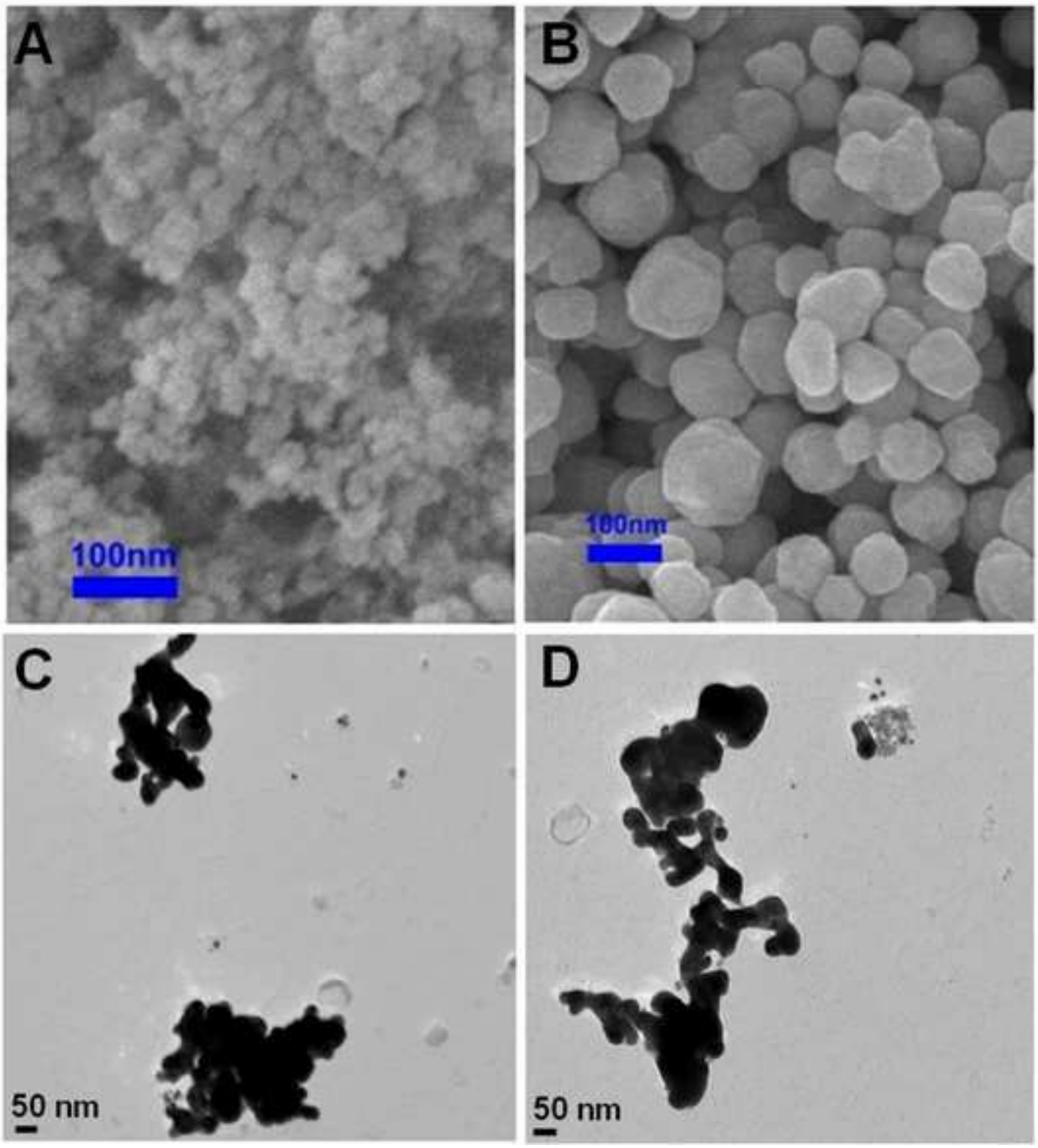

Figure 2

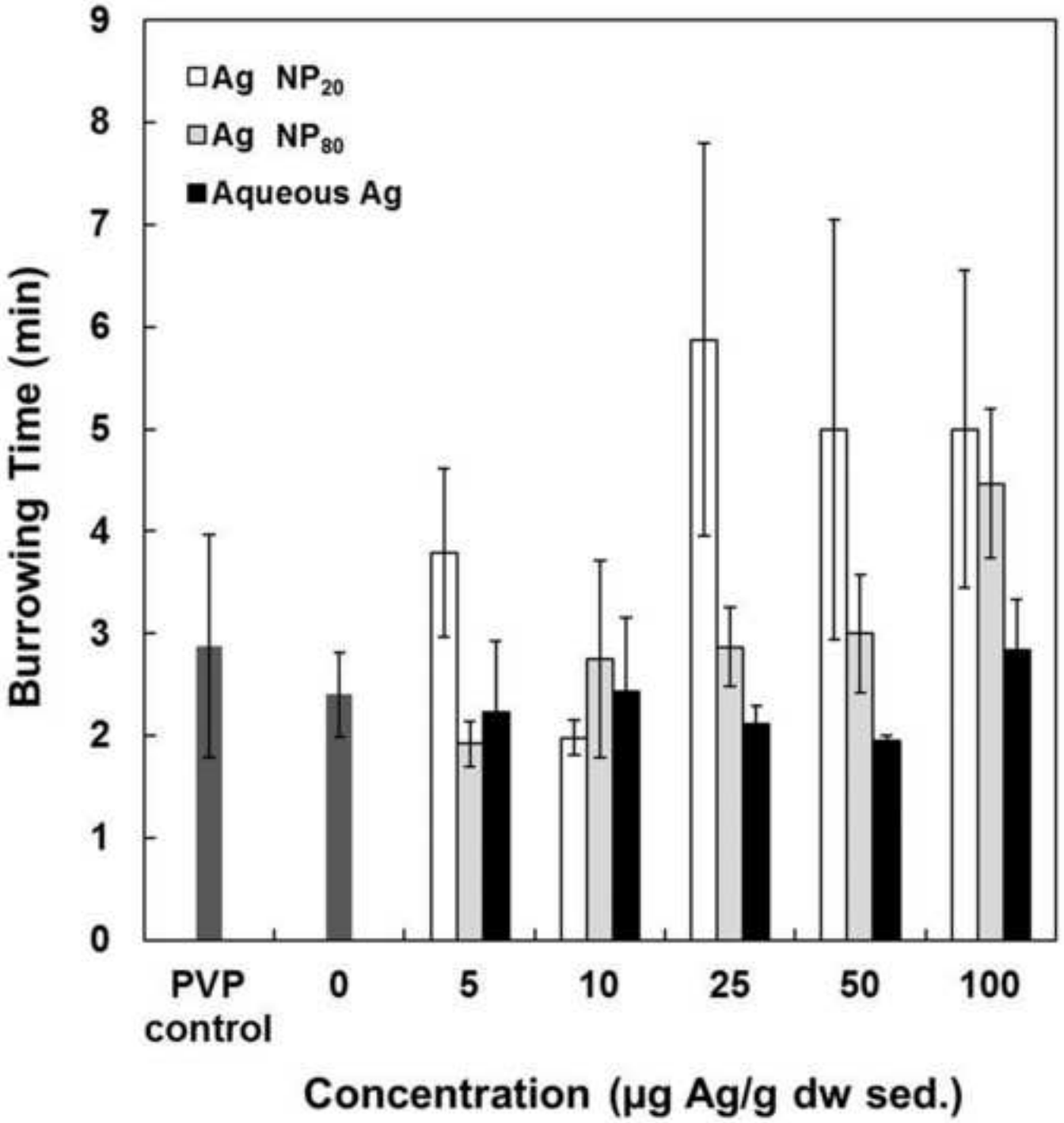
Ag NP20
Ag NP80
Aqueous Ag
Burrowing Time (min)
0
1
2
3
4
5
6
7
8
9
PVP control
0
5
10
25
50
100
Concentration (µg Ag/g dw sed.)

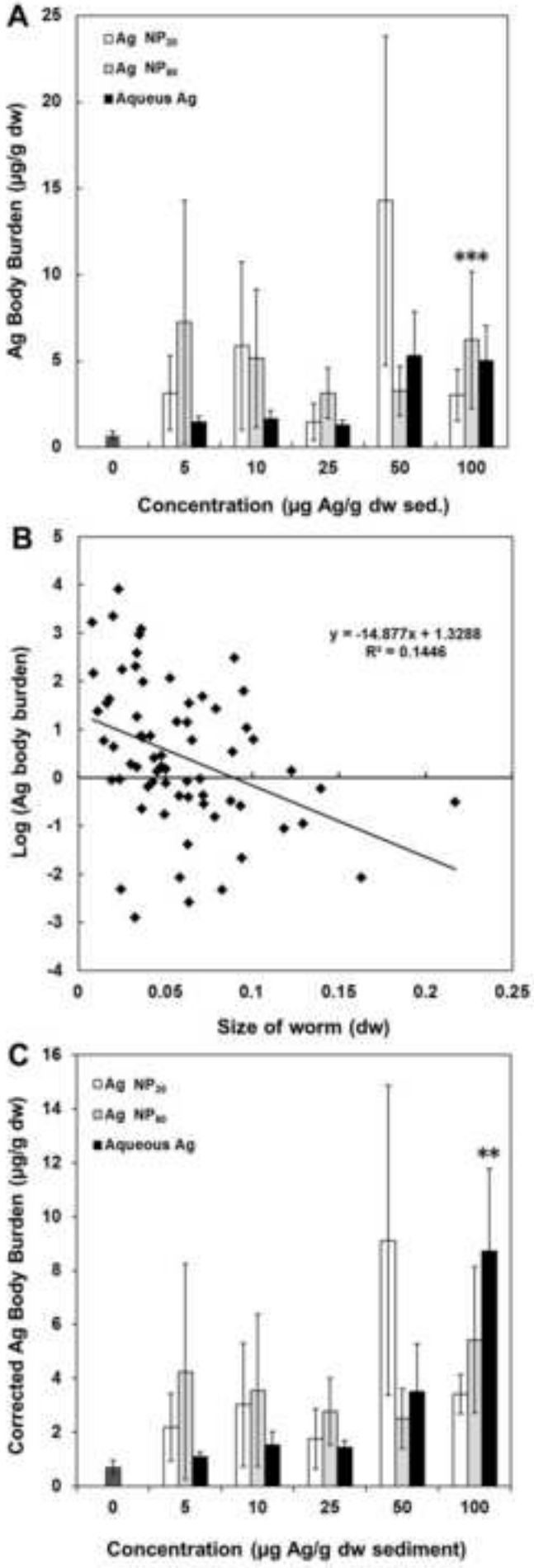

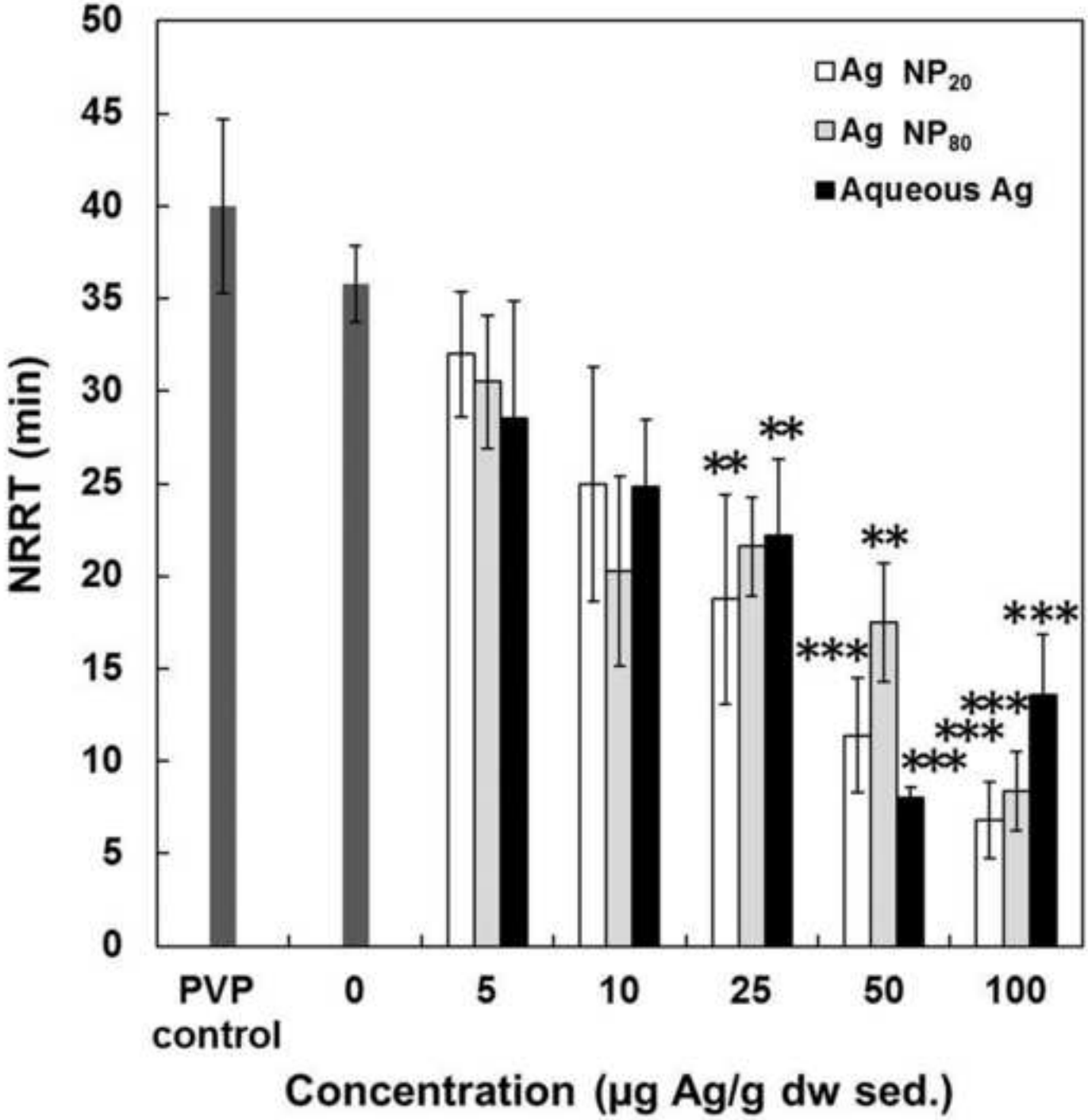

Figure 5

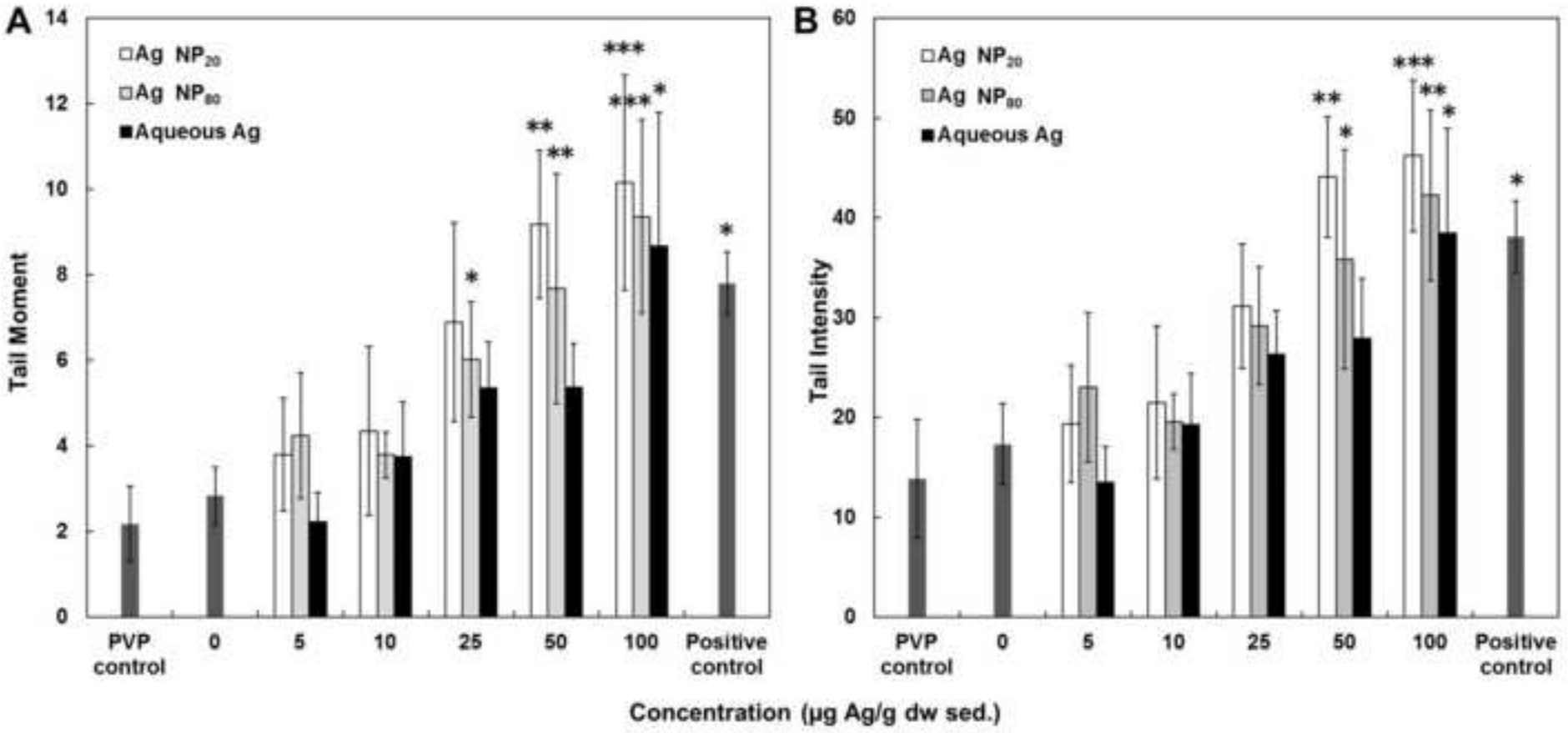
A
B
Ag NP20
Ag NP80
Aqueous Ag
Tail Moment
Tail Intensity
PVP control
0
5
10
25
50
100
Positive control
Concentration (µg Ag/g dw sed.)